

Effect of Radiation on Free Convection Flow of Non-Newtonian Power-Law Fluids Along a Power-Law Stretching Sheet

M. A. Samad, M. R. Hossain and D. Kumar

Department of Mathematics, University of Dhaka, Dhaka-1000, Bangladesh

Received on 03. 04. 2012. Accepted for Published on 16.07.2012

Abstract

An analysis is carried out to investigate the effects of MHD free convection heat transfer of power-law non-Newtonian fluids along a stretching sheet. This has been done under the simultaneous action of suction, thermal radiation and uniform transverse magnetic field. The stretching sheet is assumed to continuously moving with a power-law velocity and maintaining a uniform surface heat flux. The governing nonlinear partial differential equations are transformed into a system of nonlinear ordinary differential equations using appropriate similarity transformations. The resulting non-linear equations are solved numerically using Nachtsheim-Swigert shooting iterative technique along with sixth order Runge-Kutta integration scheme. Numerical results for the non-dimensional velocity and temperature profiles are shown graphically and discussed. The effects of skin-friction coefficient and the local Nusselt number which are of physical and engineering interest are studied and presented in the form of tables for the variation of different physically important parameters. A comparison of the present study is also performed with the previously published work and found excellent agreement.

Keywords: MHD, Power-law fluid, Radiation, Stretching sheet, Free convection, Surface heat flux

I. Introduction

The study of MHD flow of an electrically conducting fluid on stretching sheet becomes industrially important matter due to its many engineering and physical applications in modern metallurgical and metal-working process. Hot rolling, drawings of plastic films and artificial fibers, glass fiber production, metal extrusion are examples of such physical applications. Many manufacturing processes involve the cooling of continuous sheets or filaments by drawing them through a quiescent fluid which are stretched during the drawing process. The final product of required characteristics depend to a great extent on the rate of cooling which can be controlled by drawing such sheets in an electrically conducting fluid and subject to magnetic field. Sakiadis¹, first presented boundary layer flow over a continuous solid surface moving with constant speed. Elbasha² investigated heat transfer over a stretching surface with variable and uniform surface heat flux subject to injection and suction. Vajravelu *et al.*³ studied the convective heat transfer in an electrically conducting fluid near an isothermal stretching sheet and they studied the effect of internal heat generation or absorption.

The study of non-Newtonian fluid flow and heat transfer over a stretched surface gets attention due to a numerous industrially important fluids exhibit non linear relationship between shear stress and rate of strain such as polymer solution, molten plastics, pulps, paints, and foods. Rajgopal *et al.*⁵ studied flow of viscoelastic fluid over stretching sheet. Gupta *et al.*⁶ extended the problem to study heat transfer, and Datti *et al.*⁷ analyzed the problem over a non-isothermal stretching sheet. The MHD boundary layer flow over a continuously moving plate for a micropolar fluid has been studied by Rahman *et al.*⁸, and Arabawy⁹. Several authors (e.g. Anderson *et al.*¹⁰, and Mahmoud *et al.*¹¹) adopted the non-linearity

relation as power-law dependency of shear stress on rate of strain. Recently, Chen⁴ studied the effect of magnetic field and suction/injection on the flow of power-law non-Newtonian fluid over a power-law stretched sheet subject to a surface heat flux.

All the above investigations are restricted to MHD flow and heat transfer problems. However, of late, the radiation effect on MHD flow and heat transfer problems has become more important industrially. Many processes in engineering areas occur at high temperatures and knowledge of radiation heat transfer becomes very important for the design of the pertinent equipment. Nuclear power plants, gas turbines and the various propulsion devices for aircrafts, missiles, satellites, and space vehicles are examples of such engineering areas. There are various kinds of high temperature systems such as a heat exchanger and an internal combustor, in which the radiation may not be negligible in comparison with the conductive and convective heat transfer during combustion of a hydrocarbon fuel and the particles such as soot and coal suspended in a hot gas flow absorb, emit and scatter the radiation. The interaction of radiation with hydromagnetic flow has become industrially more prominent in the processes wherever high temperatures occur. Makinde¹² analyzed free convection flow with thermal radiation and mass transfer past a moving vertical porous plate. Chamkha *et al.*¹³ analyzed radiation effects on free convection flow past a semi-infinite vertical plate. Abo-Eldahab *et al.*¹⁴ studied radiation effect on heat transfer of a micropolar fluid through a porous medium

In this present work, the effect on MHD free convective heat transfer of power-law non-Newtonian fluids along a power-law stretching sheet in the presence of radiation with uniform surface heat flux have been investigated. The present study is a more generalized form of the previous study performed by Chen⁴. The effects of free convection and radiation have been accomplished which were not considered in the work of Chen⁴. A comparison of the present study is also performed with Chen⁴ and found excellent agreement.

* Correspondence author : E-mail: sanwar@univdhaka.edu

Governing Equations

Let us consider a steady two dimensional MHD free convection laminar boundary layer flow of a viscous incompressible and electrically conducting fluid obeying the power-law model along a permeable stretching sheet under the influence of thermal radiation. Introducing the Cartesian coordinate system, the X-axis is taken along the stretching sheet in the vertically upward direction and the Y-axis is taken as the normal to the sheet. Two equal and opposite forces are introduced along the X-axis, so that the sheet is stretched. This continuous sheet is assumed to move with a velocity according to a power-law form, i.e. $u_w = Cx^p$, and be subject to a surface heat flux. The ambient temperature of the flow is T_∞ . The fluid is considered to be gray, absorbing-emitting radiation but non-scattering medium and the Rosseland approximation is used to describe the radiative heat flux in the energy equation. The radiative heat flux in the X-direction is considered negligible in the comparison to the Y-direction. A strong magnetic field is applied in the Y-direction. Here, the effect of the induced magnetic field can be neglected in comparison to the applied magnetic field. The electrical current flowing in the fluid gives rise to an induced magnetic field if the fluid were an electrical insulator, but here the fluid is considered to be electrically conducting.

Hence, only the applied magnetic field B plays a role which gives rise to magnetic forces in the X-direction. Under the above assumptions, the governing boundary layer equations are:

$$\frac{\partial u}{\partial x} + \frac{\partial v}{\partial y} = 0 \quad (1)$$

$$u \frac{\partial u}{\partial x} + v \frac{\partial u}{\partial y} = \frac{\kappa}{\rho} \frac{\partial}{\partial y} \left(\left| \frac{\partial u}{\partial y} \right|^{n-1} \frac{\partial u}{\partial y} \right) + g\beta(T - T_\infty) - \frac{\sigma B^2 u}{\rho} \quad (2)$$

$$u \frac{\partial T}{\partial x} + v \frac{\partial T}{\partial y} = \alpha \frac{\partial^2 T}{\partial y^2} - \frac{1}{\rho c_p} \frac{\partial q_r}{\partial y} \quad (3)$$

The radiative heat flux q_r is described by the Rosseland approximation such that,

$$q_r = -\frac{4\sigma_1}{3k_1} \frac{\partial T^4}{\partial y} \quad (4)$$

where, σ_1 is the Stefan-Boltzman constant and k_1 is the Rosseland mean absorption coefficient. It is assumed that the temperature difference within the flow is sufficiently small such that T^4 can be expressed in a Taylor series about the free stream temperature T_∞ and then neglecting higher-order terms. This results in the following approximation:

$$T^4 \approx 4T_\infty^3 T - 3T_\infty^4 \quad (5)$$

Using (4) and (5) in the last term of equation (3), the following relation can be obtained,

$$\frac{\partial q_r}{\partial y} = -\frac{16\sigma_1 T_\infty^3}{3k_1} \frac{\partial T}{\partial y} \quad (6)$$

Introducing q_r in equation (3), the governing boundary layer equations can be written as:

$$\frac{\partial u}{\partial x} + \frac{\partial v}{\partial y} = 0 \quad (7)$$

$$u \frac{\partial u}{\partial x} + v \frac{\partial u}{\partial y} = \frac{\kappa}{\rho} \frac{\partial}{\partial y} \left(\left| \frac{\partial u}{\partial y} \right|^{n-1} \frac{\partial u}{\partial y} \right) + g\beta(T - T_\infty) - \frac{\sigma B^2 u}{\rho} \quad (8)$$

$$u \frac{\partial T}{\partial x} + v \frac{\partial T}{\partial y} = \alpha \frac{\partial^2 T}{\partial y^2} + \frac{16\sigma_1 T_\infty^3}{3\rho c_p k_1} \frac{\partial T}{\partial y} \quad (9)$$

The appropriate boundary conditions are:

$$\left. \begin{array}{l} u_w = Cx^p, \quad v = v_w, \quad \partial T / \partial y = -q_w / \kappa \quad \text{at } y = 0, \quad v = 0 \\ u_w \rightarrow 0, \quad T \rightarrow T_\infty \quad \text{as } y \rightarrow \infty \end{array} \right\} \quad (10)$$

where u and v are the velocity components, K is the consistency coefficient, c_p is the specific heat at constant pressure, $B(x)$ is the magnetic field, T is the temperature of the fluid layer, g is the acceleration due to gravity, β is the volumetric coefficient of thermal expansion, σ is the electric conductivity, ρ is the density of the fluid, α is the thermal diffusivity, k is the thermal conductivity of the fluid, n is the flow behavior index, and q_r is the radiative heat flux. v_w is the velocity component at the wall having positive value to indicate suction and negative value for injection, q_w is surface heat flux. The power index p indicates surface is accelerated or decelerated for positive and negative values respectively.

II. Similarity Analysis

In order to obtain a similarity solution of the problem, a similarity parameter $\delta(x)$ and the following dimensionless variables⁴ are introduced such that $\delta(x)$ is a length scale.

$$\eta = \frac{y}{\delta(x)} = \left(\frac{c^{2-n} x}{\kappa/\rho} \right)^{1/(n+1)} \quad (11)$$

$$\psi = \left(\frac{c^{1-2n}}{\kappa/\rho} \right)^{-1/(n+1)} x^{(p(2n-1)+1)/(n+1)} f(\eta) \quad (12)$$

$$\phi(\eta) = \frac{(T - T_\infty) \kappa c^{1/(n+1)}}{q_w \kappa} \quad (13)$$

where ψ is the stream function, η is the dimensionless distance normal to the sheet, f is the dimensionless stream function, and ϕ is the dimensionless fluid temperature. Using the transformations from equations (11) to (13) in equations (8) to (9), we obtain the following dimensionless equations as,

$$\left(|f'|^{n-1} f'' \right)' + \frac{p(2n-1)+1}{(n+1)} f f'' - p(f')^2 - M f' + \lambda \phi = 0 \tag{14}$$

$$\frac{3n+4}{3n+1} \phi'' + \frac{p(2n-1)+1}{(n+1)} f \phi' + \frac{p(2-n)-1}{(n+1)} f' \phi = 0 \tag{15}$$

The transformed boundary conditions are,

$$\left. \begin{aligned} f=1, \quad f' = \frac{n-1}{p(2n-1)+1} f_{iw}, \quad \phi' = -1 \quad \text{at } \eta=0 \\ f=0, \quad \phi=0 \quad \text{at } \eta=\infty \end{aligned} \right\} \tag{16}$$

where, $M = \frac{\sigma B^2 x}{\rho u_w}$ is the magnetic field parameter, $Pr = \frac{\rho u_w}{\alpha} Re_x^{-1/(n+1)}$ is the generalized Prandtl number, $N = \frac{h k_1}{4 \epsilon_1 T_2^3}$ is the radiation number, $f_{iw} = -\frac{u_w}{u_w} Re_x^{1/(n+1)}$ is the suction parameter, $\lambda = \frac{\sigma r}{Re_x^{1/(n+1)}} = \frac{\sigma \beta (g_w / k) x^2}{u_w^2} Re_x^{-1/(n+1)}$ is the buoyancy parameter and $Re_x = \frac{\rho u_w^2 x^{2n+1}}{\mu}$ is the local Reynolds number.

Here, it can be noted that the magnetic field strength B should be proportional to x to the power of $(p-1)/2$ to eliminate the dependence of M on x , i.e. $B(x) = B_0 x^{(p-1)/2}$, where B_0 is a constant. The parameters of engineering interest for the present problem are skin friction coefficient (C_f) and local Nusselt number (Nu_x), which indicate physically wall shear stress and local wall heat transfer rate respectively. The skin friction coefficient (C_f) is given by,

$$C_f = \frac{\tau_w}{\frac{1}{2} \rho u_w^2} \tag{17}$$

or, $Re_x^{1/(n+1)} C_f = 2 |f'''(0)|^{n-1} f'''(0)$

And the local Nusselt number Nu_x is defined as,

$$Nu_x = \frac{h x}{k} = \frac{Re_x^{1/(n+1)}}{\phi(0)} \tag{18}$$

or, $Nu_x Re_x^{-1/(n+1)} = 1/\phi(0)$

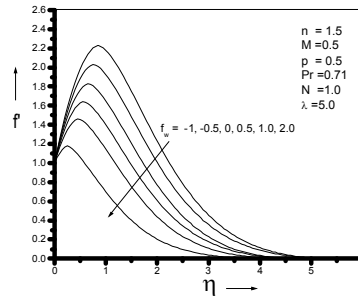
Thus from equation (17) and (18), we see that the skin friction coefficient C_f and local Nusselt number Nu_x are proportional to $2|f'''(0)|^{n-1} f'''(0)$ and $1/\phi(0)$ respectively.

III. Results and Discussion

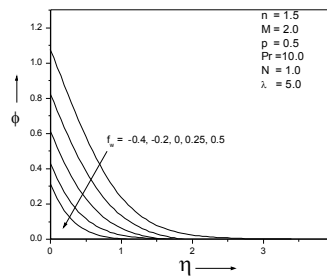
The system of transformed governing equations (14)-(15) is solved numerically using Nachtsheim-Swigert¹⁵ shooting iterative technique along with sixth order Runge-

Kutta integration scheme. Now in order to discuss the results, we solve the system (14)-(15) for different physically important parameters and carry out the discussion how these parameters do effect on the velocity and temperature of the flow field.

The effect of the suction on the velocity and temperature field are shown in Fig.1(a) and Fig.1(b) respectively. The velocity decreases with the increase of suction parameter. It indicates the fact that for a fluid with higher suction, the velocity of the fluid particle is low. For $f_{iw} = 2.0$, the pickiness of the curve is very high to indicate the fact that the velocity stabilizes very quickly (see Fig.1(a)) near the stretching sheet. The negative value of f_{iw} indicates injection. For $f_{iw} = -1.0$, the velocity increases at first due to high buoyant force ($\lambda = 5.0$). The temperature profiles in Fig.1(b) shows that the temperature decreases with the increase of suction parameter (f_{iw}).



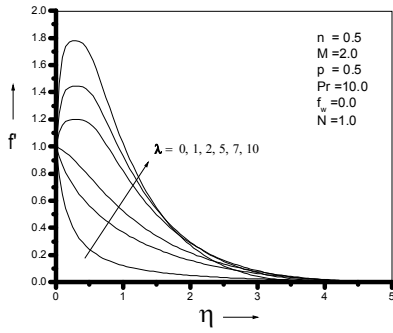
1(a)



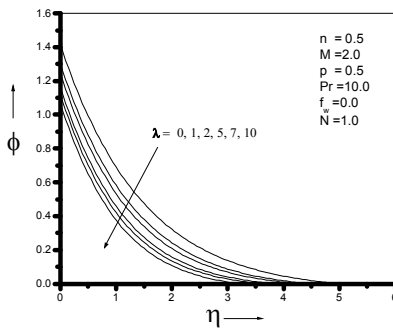
1(b)

Fig. 1. Suction parameter (f_{iw}) effect on (a) velocity and (b) temperature profile .

Fig.2(a) shows the effect on the velocity field, as velocity increases with the increase of the buoyancy parameter (λ). The velocity increases quite rapidly for $\lambda = 5.0, 7.0, 10.0$ at first near the stretching sheet and then decreases monotonically. On the other hand Fig.2(b) shows the effect of buoyancy parameter on the temperature field. The temperature decreases as the buoyancy



2(a)



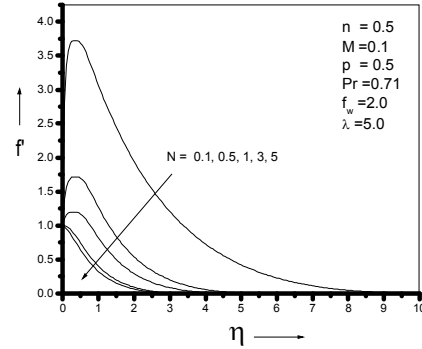
2(b)

Fig. 2. Buoyancy parameter (λ) effect on (a) velocity and (b) temperature profile .

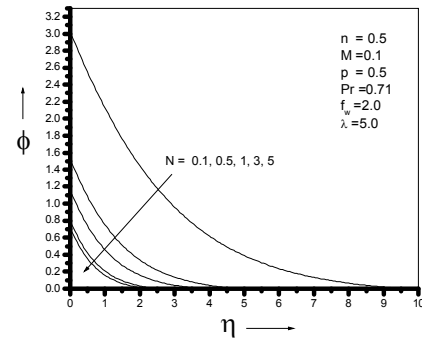
parameter (λ) increases. From Fig. 2(a) it can be observed that for larger λ the velocity profiles stabilize quickly and near $\eta = 2.0$, there is a cross flow.

In Fig.3(a) and Fig.3(b), the effect of radiation number (N) on velocity and temperature profiles is shown respectively. It is quite clear from both the graphs that velocity and temperature profiles decrease as the radiation parameter (N) increases. However, the velocity profiles rise near the stretching sheet for all values of N . Also it clears the fact that the velocity profile and wall temperature decreases very rapidly for $N \geq 1.0$ to indicate that the radiation effect can be used to control the velocity and temperature of the boundary layer.

Fig.4 and Fig.5 reveals that the velocity decreases whereas temperature profile increases as magnetic number (M) increases. However, from Fig.4(a) and Fig.5(a), it can be seen that there is a sharp rise in velocity profiles near the surface. Magnetic field lines act as a string to retard the motion of the fluid. The consequence of which is to increase the rate of heat transfer.



3(a)

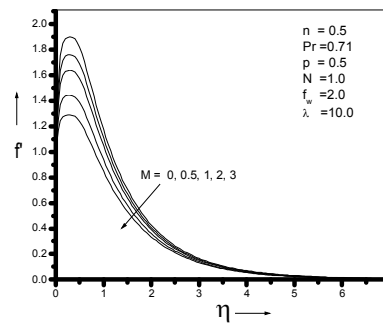


3(b)

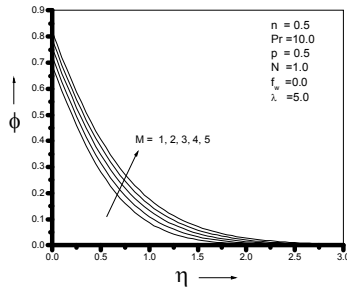
Fig. 3. Radiation number (N) effect on (a) velocity and (b) temperature profile .

Fig.4(b) and Fig.5(b) show that, the effect of magnetic parameter (M) on temperature profiles is more noticeable for the pseudo-plastic fluids than the dilatant fluids.

Fig.6(a) and Fig.6(b) display the effect of Prandtl number (Pr) on velocity, and temperature respectively. From both the figure we observe that the velocity and temperature profiles decrease with the increase of Prandtl number (Pr).

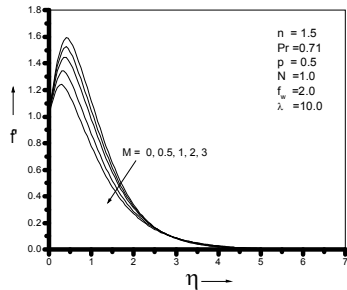


4(a)

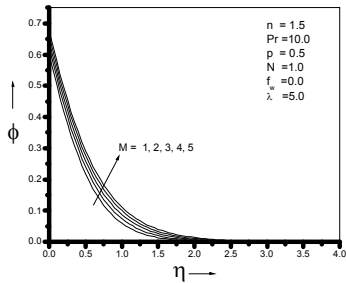


4(b)

Fig. 4. Magnetic field parameter (M) effect on (a) velocity and (b) temperature profile for $n = 0.5$.

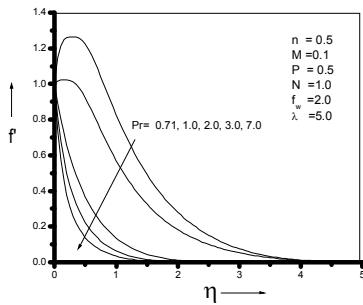


5(a)

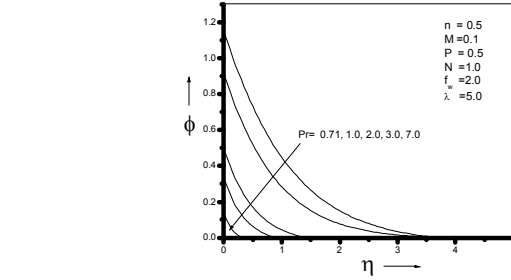


5(b)

Fig. 5. Magnetic field parameter (M) effect on (a) velocity and (b) temperature profile for $n = 1.5$.



6(a)



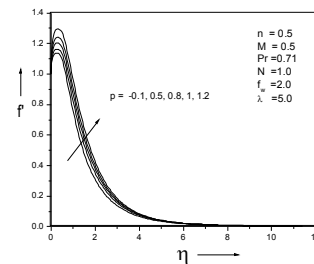
6(b)

Fig. 6. Prandtl number (Pr) effect on (a) velocity and (b) temperature profile.

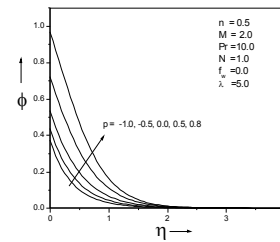
From Fig.6(b) it is clear that for small Pr wall temperature is very high compared to larger values.

The effect of velocity index on velocity and temperature profiles is shown in the Fig.7 and Fig.8 respectively. Velocity and temperature increases with increasing velocity index (β) for pseudo-plastic fluids. The dilatant fluids show completely opposite behavior which are visible from Fig.8(a) and Fig.8(b). The effect of velocity index (β) on temperature profiles is more noticeable in case of pseudo-plastics.

The effect of power-law fluid index (n) on the velocity and temperature field has shown for accelerating ($\beta = 1$) and decelerating ($\beta = -0.3$) surface flows in Fig.9 and Fig.10 respectively. Fig.9(a) illustrates that the velocity profile decreases with the increase of power-law fluid index (n) for flows where the surface is accelerated. However, the opposite

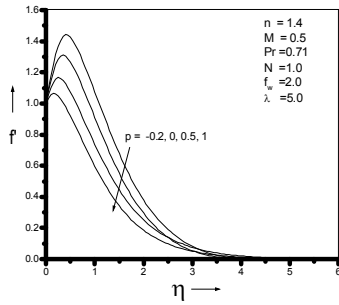


7(a)

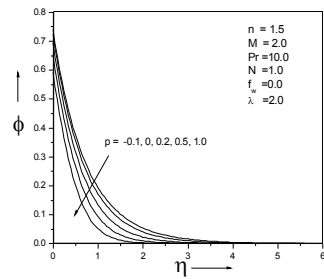


7(b)

Fig. 7. Velocity index (β) effect on (a) velocity and (b) temperature profile.

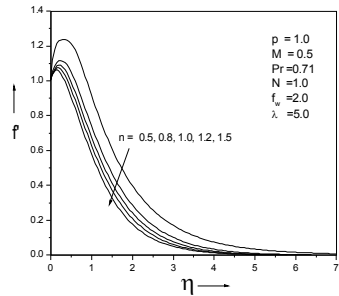


8(a)

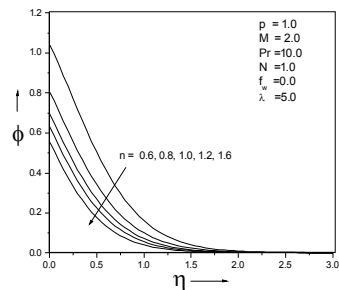


8(b)

Fig. 8. Velocity index (p) effect on (a) velocity and (b) temperature profile.



9(a)



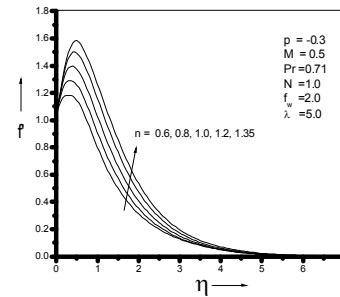
9(b)

Fig. 9. Power-law fluid index (n) effect on (a) velocity and (b) temperature profile for $p = 1$.

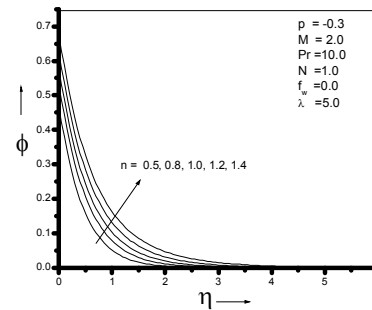
trend is quite clear for decelerated surface from Fig.10(a).The temperature profiles also decrease with the increase of power-law fluid index (n) for $p = 1$ and increase for $p = -0.3$. Comparing Fig.9(b) and Fig.10(b), the effect of power-law fluid index (n) is more noticeable in case of accelerated surface flows.

To assess the accuracy of our code, we calculated the skin friction coefficient and the local heat transfer rate. We compared these physically important parameters with that of Chen⁴ for forced convection (i.e. $\lambda = 0$) and found excellent agreement (see Table-1).

The effect of surface velocity index p on skin friction coefficient C_f and local Nusselt number Nu_x has been showed in the Fig.11. The parameter C_f decreases as the index p increases.



10(a)



10(b)

Fig. 10. Power-law fluid index (n) effect on (a) velocity and (b) temperature profile for $p = -0.3$.

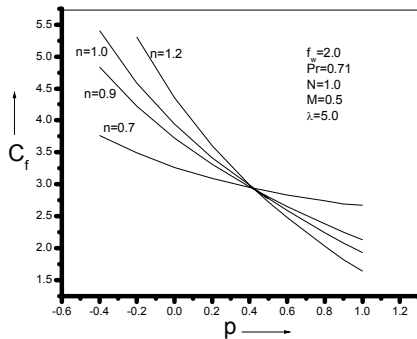
It is interesting to note that for smaller values of p , C_f increases with the increase of n , while the opposite trend is visible for larger p . The local heat transfer rate on the other hand increases with n for larger p and the trend is reversed for a smaller p .

The effect of Prandtl number Pr on skin friction coefficient C_f and local Nusselt number Nu_x has been showed in the figures (Fig.12). The skin friction coefficient C_f decreases with Prandtl number Pr for fixed n and ρ . For accelerated surface ($\rho = 1.0$), C_f decreases with n and increases for decelerated surface ($\rho = -0.5$). The effect of Prandtl number Pr on heat transfer rate has shown for the range $0.1 \leq Pr \leq 100$. The local Nusselt number Nu_x increases with the increase of Pr and fixed values of n . For accelerated surface ($\rho = 1.0$), the heat transfer rate increases with n , while opposite trend is visible for decelerated surface ($\rho = -0.5$).

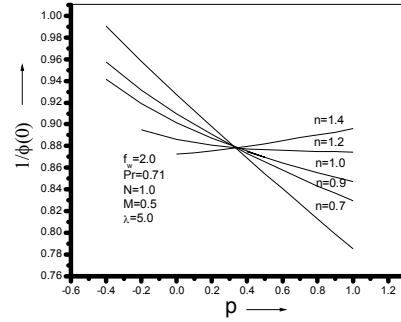
Table. 1*. Comparison of $Re_x^{1/(n+1)} C_f$ and $Nu_x Re_x^{-1/(n+1)}$

Parameters			$Re_x^{1/(n+1)} C_f$		$Nu_x Re_x^{-1/(n+1)}$	
n	M	f_w	Chen ⁴	Present study	Chen ⁴	Present study
0.5	1	-0.2	-2.472213	-2.4723340	0.791413	0.7913201
		0.0	-2.633241	-2.6334386	1.346116	1.3461035
		0.6	-3.213067	-3.2137484	3.683003	3.6833107
1.0	5	-0.2	-3.881351	-3.8813143	0.367234	0.3679528
		0.6	-4.608094	-4.6078741	3.528467	3.5287845
		0.0	-2.519363	-2.5193782	1.578424	1.5785883
1.5	1	-0.2	-2.323803	-2.3238161	1.019734	1.0198238
		0.6	-3.198565	-3.1985827	3.866662	3.8672224
		0.0	-2.519363	-2.5193782	1.578424	1.5785883
1.9	5	-0.2	-4.529439	-4.5294577	0.692476	0.6935165
		0.6	-5.366930	-5.3668243	3.754876	3.7553935
		0.0	-2.412287	-2.4121919	1.689593	1.6902300
1	0	-0.2	-1.073300	-1.0734818	1.278189	1.2783778
		0.6	-2.107985	-2.1080359	1.180071	1.1812444

* $\rho = 0.5, Pr = 5, \lambda = 0$

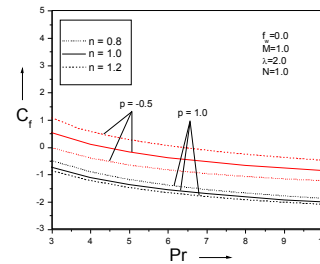


11(a)

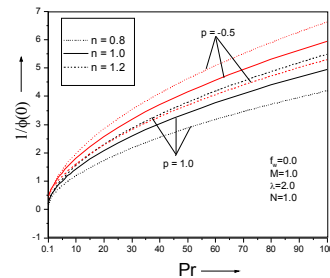


11(b)

Fig. 11. Velocity index (ρ) effect on (a) skin friction coefficient C_f and (b) local Nusselt number Nu_x



12(a)



12(b)

Fig. 12. Prandtl number (Pr) effect on (a) skin friction coefficient C_f and (b) local Nusselt number Nu_x

Table 2**. Effect of λ , n , M and f_w on parameters, C_f and Nu_x

Parameters			Free convection $\lambda = 5$		Free convection with radiation $\lambda = 2, N = 1.0$	
n	M	f_w	C_f	Nu_x	C_f	Nu_x
0.5	0	0.0	-0.0039949	1.6485333	-0.2523604	1.0525760
		0.6	-1.9880262	3.8283292	-1.7551101	1.8930113
1	0	0.0	-0.9537600	1.5622031	-1.2342641	0.9673900
		0.6	-2.7677778	3.7458588	-2.5963237	1.8082045
5	-0.2	0.0	-1.7028318	0.9014518	-2.4497347	0.5864786
		0.6	-2.6929857	1.3167073	-2.9747175	0.7650920
1.0	0	0.0	-4.2481893	3.5793664	-4.1654224	1.6581498
		0.6	-1.0942870	1.3309287	0.4671101	0.9446971
1	-0.2	0.0	0.0688451	1.8094812	-0.0965771	1.1483695
		0.6	-1.8255929	3.9683776	-1.5925688	1.9826609
5	-0.2	0.0	0.2153344	1.2452110	-0.4486410	0.8623030
		0.6	-0.8550189	1.7176044	-1.0463472	1.0632343
1.5	0	0.0	-2.7399391	3.9168430	-2.5351329	1.9214060
		0.6	-1.9391421	1.0411162	-2.6737635	0.6788470
1	-0.2	0.0	-3.0850104	1.5021815	-3.3287963	0.8762281
		0.6	-4.9383161	3.7946392	-4.8012559	1.7985942
5	0.6	0.0	0.9216363	1.4308726	0.4315933	1.0058131
		0.6	0.1514995	1.8951675	-0.0001776	1.1965294
1.9	0	0.0	-1.7421343	4.0201224	-1.5140543	2.0196631
		0.6	0.2007664	1.3317702	-0.3174142	0.9108896
1	-0.2	0.0	-0.7486714	1.7999822	-0.8985304	1.1120260
		0.6	-2.7074518	3.9957781	-2.4856369	1.9736653
5	0.6	0.0	-5.3039239	3.8831391	-5.1433146	1.8745382
		0.6	1.7102525	4.0439036	-1.4913180	2.0415664
1.9	0	0.0	-0.6854259	1.8429929	-0.8074195	1.1358667
		0.6	-5.5024516	3.9433525	-5.3211893	1.9118353

** $p = 0.5, Pr = 5.0$

Table-2 shows the value of C_f and Nu_x for various values of n , M and f_w with $\lambda = 5$ and $\lambda = 2, N = 1$. The increasing magnetic field decreases local heat transfer rate. As the suction parameter f_w increases the local Nusselt number increases quite significantly. The shear thinning fluid ($n < 1$) posses smaller skin friction coefficient and larger heat transfer rate. The buoyancy force is found to increase wall friction coefficient, but its effect on local Nusselt number is not noticeable.

IV. Conclusion

From the present investigation we can make the following conclusions:

1. Thermal radiation can be used effectively to control the velocity and thermal boundary layers
2. Suction stabilizes boundary layer growth.
3. The buoyancy force increases the wall friction and thus thickening the velocity boundary layer.
4. Drag of the pseudo-plastics along a stretched surface decreases as the velocity index increases.
5. A strong magnetic field can be applied to increase the wall temperature of the pseudo-plastic fluids.

6. The heat transfer rate of dilatant fluids are greater than pseudo-plastic fluids for a decelerated surface flow while the opposite behavior is visible for accelerated surface flow.

.....

1. Sakiadis B. C., 1961. Boundary Layer Behavior on Continuous Solid Surfaces: I. The Boundary Layer Equations for Two-Dimensional and Axisymmetric Flow., *AIChE J.* 7, 26-28.
2. Elbashbeshy E. M. A., 1998. Heat Transfer over a Stretching Surface with Variable Surface Heat Flux. *J. Phys. D: Appl.Phys.* 31, 1951-1954.
3. Vajravelu K. and A. Hadjinicolaou, 1997. Convective Heat Transfer in an Electrically Conducting Fluid at a Stretching Surface with Uniform Free Stream. *Internat. J. Engrg. Sci.* 35, 12-13, 1237-1244.
4. Chen C.H., 2008. Effects of Magnetic Field and Suction/Injection on Convective Heat Transfer on Non-Newtonian Power-Law Fluids Past a Power-Law Stretched Sheet with Surface Heat Flux. *Int. J. Thermal Sci.* 47, 954-961
5. Rajgopal K.R., T.Y. Na, A.S. Gupta, 1984. Flow of a Viscoelastic Fluid over a Stretching Sheet. *Rheol. Acta* 23, 213-215.
6. Dandapat B.S., A.S. Gupta, 2005. Flow and Heat Transfer in a Viscoelastic Fluid over a Stretching Sheet., *Int. J. Non-Linear Mech.* 40, 215-219.
7. Datti P.S., K.V. Prasad, M.S. Abel, A. Joshi, 2005. MHD Viscoelastic Fluid Flow over a Non-Isothermal Stretching Sheet. *Int. J. Eng. Sci.* 42, 935-946.
8. Rahman M.M., M.A. Sattar, 2006. Magnetohydrodynamic Convective Flow of a Micropolar Fluid Past a Continuously Moving Vertical Porous Plate in the Presence of Heat Generation/Absorption. *ASME J. Heat Transfer* 128,142-152.
9. El-Arabawy Hassan A.M., 2003. Effect of Suction/Injection on the Flow of a Micropolar Fluid Past a Continuously Moving Plate in the Presence of Radiation, *Int. J. Heat Mass Transfer* 46, 1471-1477
10. Anderson H.I., K.H. Bech, B.S. Dandapat, 1992. Magnetohydrodynamic Flow of a Power-Law Fluid over a Stretching Sheet. *Int. J. Non-Linear Mech.* 27, 926-936.
11. Mahmoud M.A.A. and M.A.E. Mahmoud, 2006. Analytical Solutions of Hydromagnetic Boundary Layer Flow of Non-Newtonian Power-Law Fluid Past a Continuously Moving Surface, *Acta Mech.* 181, 83-89.
12. Makinde O.D., 2005. Free Convection Flow with Thermal Radiation and Mass Transfer Past a Moving Vertical Porous Plate, *Int. Comm. Heat Mass Transfer* 32, 1411-1419
13. Chamkha A.J., H.S. Takhar and V.M. Soundalgekar, 2001. Radiation Effects on Free Convection Flow Past a Semi-Infinite Vertical Plate with Mass Transfer. *Chem.Engg.J.* 84, 335-342.
14. Abo-Eldahab E. M., A. F. Ghonaim, 2005. Radiation Effect on Heat Transfer of a Micropolar Fluid Through a Porous Medium, *App. Math. Comp.* 169, 500-510
15. Nachtsheim, P.R. and P. Swigert, 1965. Satisfaction of the Asymptotic Boundary Condition in Numerical Solution of the System of Nonlinear Equation of Boundary Layer Type. *NASA TND-3004.*